

A novel intracellular protein delivery platform based on single-protein nanocapsules

Ming Yan^{1†}, Juanjuan Du^{1†}, Zhen Gu¹, Min Liang², Yufang Hu³, Wenjun Zhang¹, Saul Priceman³, Lily Wu³, Z. Hong Zhou^{2,4}, Zheng Liu^{5*}, Tatiana Segura^{1*}, Yi Tang^{1*} and Yunfeng Lu^{1*}

An average cell contains thousands of proteins that participate in normal cellular functions, and most diseases are somehow related to the malfunctioning of one or more of these proteins. Protein therapy¹, which delivers proteins into the cell to replace the dysfunctional protein, is considered the most direct and safe approach for treating disease. However, the effectiveness of this method has been limited by its low delivery efficiency and poor stability against proteases in the cell, which digest the protein. Here, we show a novel delivery platform based on nanocapsules consisting of a protein core and a thin permeable polymeric shell that can be engineered to either degrade or remain stable at different pHs. Non-degradable capsules show long-term stability, whereas the degradable ones break down their shells, enabling the core protein to be active once inside the cells. Multiple proteins can be delivered to cells with high efficiency while maintaining low toxicity, suggesting potential applications in imaging, therapy and cosmetics fields.

The intracellular use of therapeutic proteins is of great importance in the treatment of cancers and protein deficiency diseases. However, clinical applications remain rare, partly due to the poor stability and low cellular permeability of the proteins^{1,2}. Although proteins may be translocated into cells by receptor-mediated endocytosis^{3,4}, they can become entrapped within endosomes and degraded in the lysosome rather than being released to the appropriate cellular compartment. Similarly, liposome-wrapped proteins have been shown to be transferred into the cytoplasm, but with low efficiency^{5,6}. Recently, cell-penetrating peptides (CPPs), which have been used to assist protein delivery, have shown significantly improved delivery efficiency^{7–9}. However, the stability of the proteins¹⁰, particularly against protease digestion¹¹, still hampers their use in therapeutic applications.

We report a novel intracellular delivery platform based on nanocapsules that consist of a single-protein core and thin polymer shell anchored covalently to the protein core. As illustrated in Fig. 1a, polymerizable vinyl groups are covalently linked to the protein (I). Subsequent polymerization in an aqueous solution containing monomers (1, 2) and crosslinker (3, 4) results in each protein core being wrapped in a thin polymer shell. This scheme enables the synthesis of protein nanocapsules with a non-degradable (II) or degradable (III) skin by using non-degradable (3) or degradable (4) crosslinkers, respectively. Hereinafter, the non-degradable and degradable nanocapsules are denoted nProtein and *de*-nProtein, respectively, where the prefix 'n' denotes 'nanocapsule'. Appropriate choice of the monomer, such as the cationic (2) or

neutral (1) monomers, allows precise control of surface charge. The protein cores can be chosen from a vast library of proteins, including enhanced green fluorescent protein (EGFP), horseradish peroxidase (HRP), bovine serum albumin (BSA), superoxide dismutase (SOD) and caspase-3 (CAS).

Figure 1b,c presents transmission electron microscopy (TEM; Fig. 1b) and atomic force microscopy (AFM; Fig. 1c) images of nHRP synthesized according to this process; these show that the nanocapsules are spherical, with a uniform diameter of ~15 nm, as confirmed by dynamic light scattering (DSL) measurements (Supplementary Fig. S1). Because the radius of an HRP molecule is ~5 nm, the average shell thickness is determined to be ~5 nm. Each HRP molecule was labelled with a single 1.4-nm gold nanoparticle. Most of the nanocapsules that were observed contained only a single gold nanoparticle (Fig. 1d), confirming the predicted single-protein core-shell structure. The surface charge of nanocapsules can be adjusted by varying the ratios of the cationic and neutral monomers used (Supplementary Fig. S2). It is therefore possible to readily create nanocapsules with precisely controlled size, surface charge and degradability (Supplementary Table S1). In contrast to nProteins with long-term intracellular stability and activity for small substrates, *de*-nProteins can be stripped of their shells intracellularly, enabling their core proteins to interact with macromolecular substrates (step V, Fig. 1a).

Cell transduction efficiency was studied using nEGFP and HeLa cells. Cells carrying nEGFP show significantly higher fluorescence intensity than those with native EGFP (Fig. 2a,b). Compared with CPP-assisted delivery, our strategy is clearly advantageous. At the same protein concentration, cells incubated with nanocapsules show two to three orders higher fluorescence intensities than those with TAT-EGFP fusion proteins (Fig. 2b) or antennapedia-EGFP conjugates (Supplementary Fig. S10; TAT and antennapedia are CPPs derived from HIV-Tat protein and antennapedia homeodomain, respectively). It was found that uptake of nanocapsules increased with time (Supplementary Fig. S3), concentration (Fig. 2b) and zeta potential (Fig. 2c); however, no significant impact of nanocapsule size (in the range 7.5–15.7 nm, Supplementary Fig. S4) was observed.

Incubating HeLa cells with nEGFP at 4 °C revealed a much lower cellular uptake than at 37 °C (Fig. 2d), which is consistent with results for most cationic CPPs and polymer-based nanoparticles^{12–15}. Of three endocytosis inhibitors applied (Fig. 2d), only β -cyclodextrin (β -CD) effectively inhibited nanocapsule uptake, suggesting a caveolae-mediated endocytosis pathway.

¹Department of Chemical and Biomolecular Engineering, University of California at Los Angeles, Los Angeles, California 90095, USA, ²Department of Microbiology, Immunology and Molecular Genetics, University of California at Los Angeles, Los Angeles, California 90095, USA, ³Department of Medical and Molecular Pharmacology, UCLA David Geffen School of Medicine, University of California at Los Angeles, Los Angeles, California 90095, USA, ⁴California NanoSystems Institute, University of California at Los Angeles, Los Angeles, California 90095, USA, ⁵Department of Chemical Engineering, Tsinghua University, Beijing 10084, China; [†]These authors contributed equally to this work. *e-mail: tsegura@ucla.edu; zhengliu@tsinghua.edu.cn; yitang@ucla.edu; luucla@ucla.edu

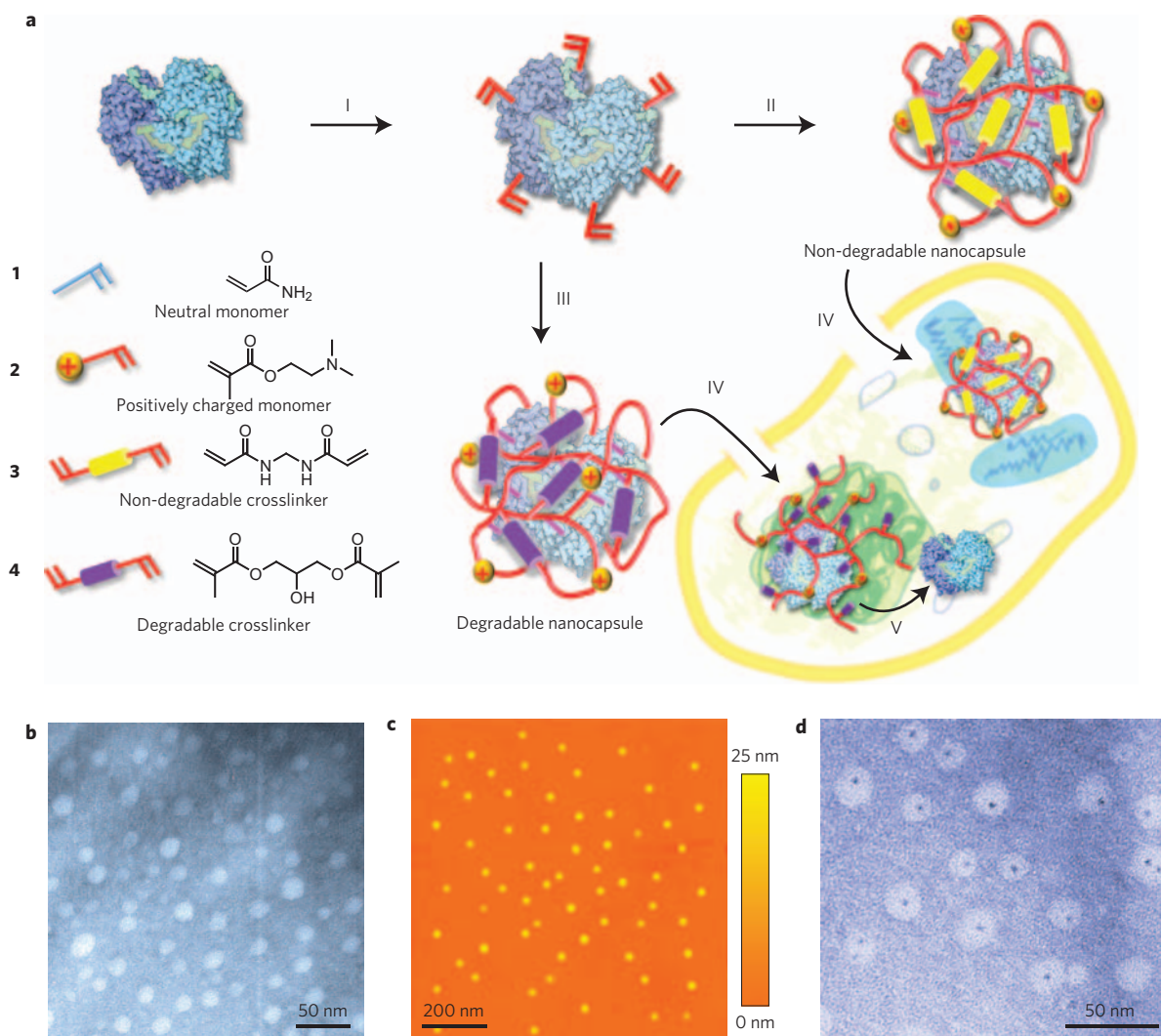


Figure 1 | Protein nanocapsules. **a**, Schematic showing the synthesis and cellular uptake of cationic single-protein nanocapsules with degradable and non-degradable polymeric shells prepared by *in situ* co-polymerization of acrylamide **1**, 2-dimethylaminoethyl methacrylate **2** and non-degradable crosslinker methylenebisacrylamide **3** or acid-degradable glycerol dimethacrylate **4**: I, formation of polymerizable proteins by conjugating polymerizable acryl groups to the protein surface; II, formation of non-degradable nanocapsules from **1**, **2** and **3**; III, formation of degradable nanocapsules from **1**, **2** and **4**; IV, cellular uptake of the degradable or non-degradable nanocapsules via endocytosis; V, shells of degradable nanocapsules break down after internalization to release the protein cargoes, allowing them to interact with large molecular substrates. **b,c**, Representative TEM (**b**) and AFM (**c**) images of the HRP nanocapsules. **d**, TEM image of nanocapsules containing a single 1.4-nm gold-quantum-dot-labelled HRP core confirms the formation of a single-core nanoscale architecture.

Magnified images consistently show an inhomogeneous distribution of the nanocapsules in the cells (Fig. 2e). A TEM image of cells transfected with gold-labelled nHRP reveals clusters of the nanocapsules with contour similar to that of endosomes (green arrow) and dispersion of single nanocapsules within the cytosol (red arrow, Fig. 2f). Moreover, endosomal and lysosomal staining of the cells incubated with rhodamine-B-labelled nHRP reveals colocalization of nHRP with early endosomes and lysosome after 30 min, with gradual release to the cytosol (Supplementary Fig. S13), possibly by means of the ‘proton-sponge’ effect¹⁶.

This method can be generalized to multiple protein delivery while maintaining low toxicity. Figure 2e shows fluorescence images of HeLa cells simultaneously internalizing nEGFP (green), rhodamine-B-labelled nHRP (red) and NIR-667-labelled nBSA (blue). Such a multiple protein delivery method has great potential for therapies in which proteins act synergistically or in tandem^{17,18}. Figure 2g compares the viability of HeLa cells after exposure to different nEGFP and native EGFP concentrations (Supplementary Fig. S5), and suggests similar cytotoxicities for both nEGFP and

native EGFP. Following exposure to nanocapsules at a maximum concentration of 1.67 μM , cell viability decreased by only 15%.

Proteases are commonly present in a physiological environment in which proteins are readily degraded. However, the polymer shell protects the protein core from proteolysis well. Figure 3a compares fluorescence intensities of native EGFP and nEGFP after exposure to proteases (trypsin and α -chymotrypsin) at a concentration of 1 mg ml⁻¹, at 50 °C for 3 h. The native EGFP only retained 60% of its original fluorescence intensity, whereas the nanocapsules retained more than 90%. Intracellular stability was examined by comparing the temporal fluorescence intensities after transduction (Fig. 3b). Inevitably, the cellular fluorescence decreased with time as a result of cell propagation; nevertheless, the stability of nEGFP is significantly improved over that of TAT-EGFP.

The *in vivo* stability of the nanocapsules was examined by injecting nude mice intraperitoneally with 0.2 mg nEGFP or native EGFP. Organ sections showed intense fluorescence 8 h after injection, which remained high even after 50 h (Fig. 3c), whereas signals in the control mice remained at background levels. To examine the

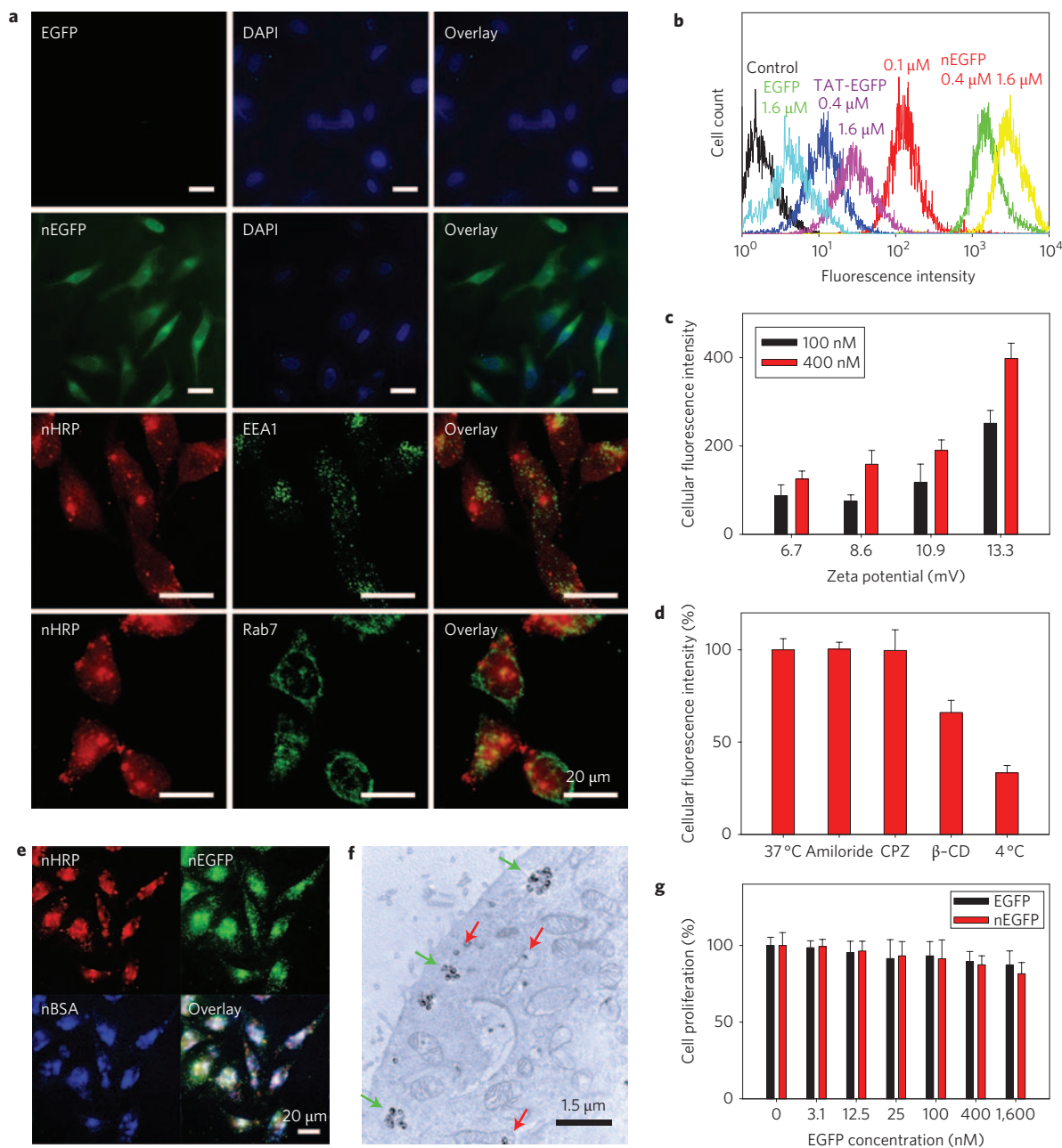


Figure 2 | Transduction efficiency of protein nanocapsules in HeLa cells. **a**, Fluorescent images show the uptake of nEGFP and rhodamine-labelled nHRP but not native EGFP after incubation for 3 h. Cells were counter-stained with DAPI (for nuclei), EEA1 (for early endosomes) or Rab7 (for lysosomes). **b**, Fluorescence-assisted cell sorting of HeLa cells incubated with different concentrations of nEGFP (11.7 nm, zeta potential 10.9 mV), TAT-EGFP fusion proteins or native EGFP. **c**, Uptake of nEGFP by HeLa cells increased with zeta potential after 3 h. **d**, Average cellular fluorescence intensity of HeLa cells at different temperatures and in the presence of three different endocytosis inhibitors: Amiloride, CPZ and β -cyclodextrin (β -CD). Fluorescence intensity is normalized to cells incubated with nEGFP at 37 °C. **e**, Confocal images of HeLa cells after transduction of rhodamine-B-labelled nHRP (red), nEGFP (green), and NIR-667-labelled nBSA (blue) show multiple-protein delivery. **f**, TEM image of a HeLa cell after incubation with gold quantum-dot-labelled HRP nanocapsules. Red arrows show dispersion of single nanocapsules in the cell cytosol; green arrows show clusters of nanocapsules. **g**, MTT assay showing that nEGFP has a similar cytotoxicity to native EGFP after incubation for 3 h. Data represent averages, with error bars from three independent experiments performed in triplicate.

in vivo activity of the nanocapsules, nHRP or native HRP was injected into mice and their activity within the organ sections was assessed using dihydroethidium, a fluorogenic substrate for HRP. As shown in Fig. 3c, 8 h after injection, the tissues of the nanocapsule-injected mice show intense red fluorescence, indicating that the nanocapsules are active *in vivo*.

The ability to deliver active nanocapsules with high efficiency, long-term stability and low toxicity opens a new direction for

protein therapies, imaging, tumour tracking, cosmetics and other applications. For example, the combination of indole-3-acetic acid (IAA) and HRP has recently been proposed as a potential prodrug for cancer therapy¹⁹. IAA is well tolerated in humans, and could be specifically transformed to a free radical intermediate by HRP and induce apoptosis in mammalian cells²⁰. nHRPs were first incubated with HeLa cells, which were then exposed to a chromogenic substrate. The green colour in the cell medium intensified

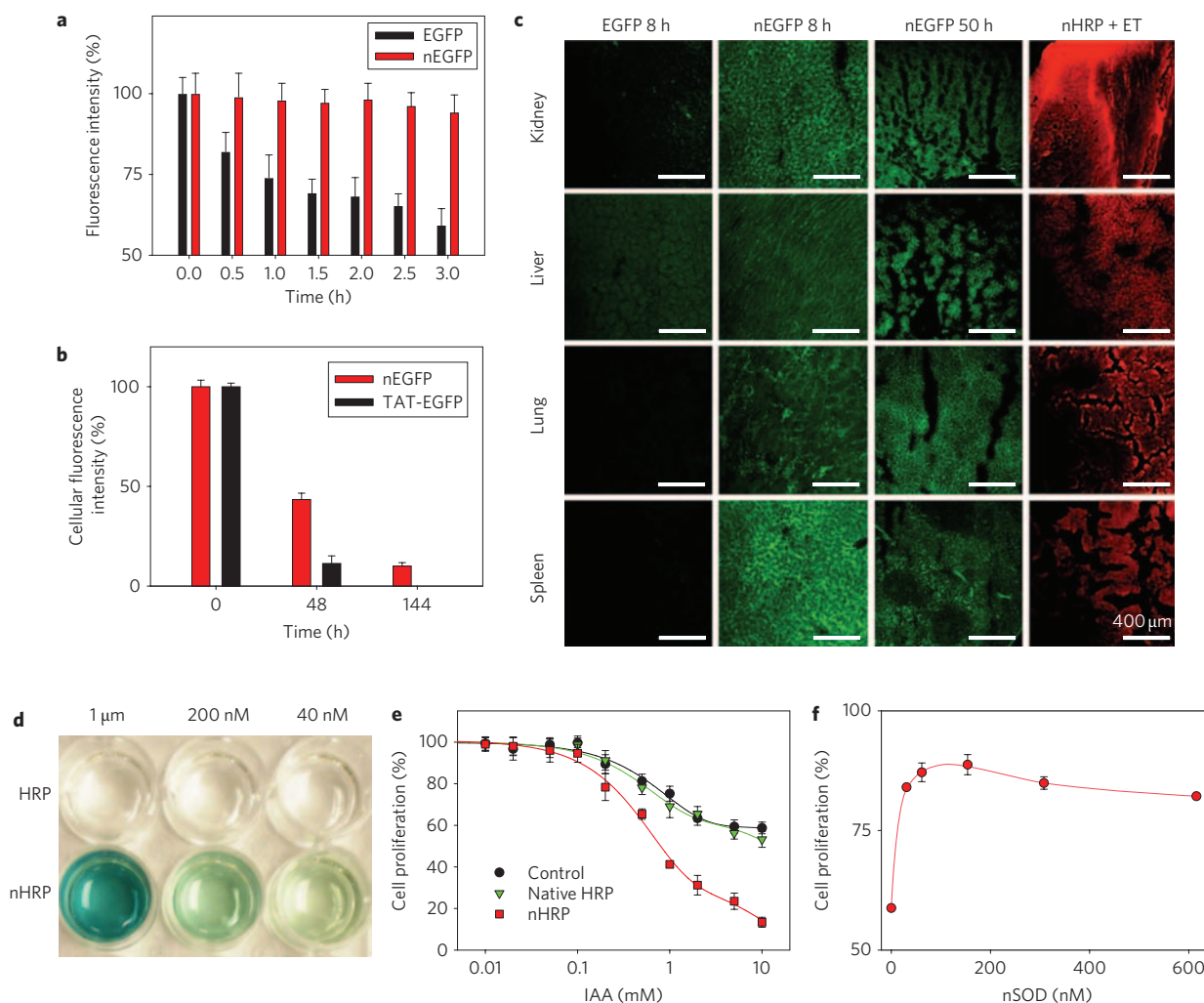


Figure 3 | Stability and activity of nanocapsules in cells and mice. **a**, Fluorescence intensity of native EGFP and nEGFP after exposure to 1 mg ml^{-1} trypsin and α -chymotrypsin at 50°C . Fluorescence intensities are normalized to native EGFP before exposure to protease. **b**, Cellular fluorescence intensity of cells after treatment with nEGFP or TAT-EGFP fusion proteins at different times. **c**, Confocal images of tissue sections of mice treated with native EGFP, nEGFP or nHRP exposed to dihydroethidium (ET). **d**, HeLa cells after incubation with native HRP or nHRP at different concentrations for 3 h, followed by phosphate buffered saline washes and incubation with 3,3',5,5'-tetramethylbenzidine (TMB) and H_2O_2 . **e**, MTT assay showing HeLa cell viability after transduction with 400 nM native HRP or nHRP and incubation with IAA for 12 h. Cell proliferation rates were normalized to untreated cells. **f**, HeLa cell viability after incubation with nSOD and paraquat. Untreated cells were used as the 100% cell proliferation control and cells treated with paraquat only were used as the 0% control. Data represent averages, with error bars from three independent experiments performed in triplicate.

with increasing nanocapsule concentration, indicating successful delivery of active HRP (Fig. 3d). Consistently, the cells incubated with the nanocapsules show rapidly decreasing cell viability with increasing IAA concentration, whereas those with native HRP perform similarly to the untreated cells (Fig. 3e), suggesting great potential for the use of nanocapsules in cancer therapies.

Similarly, superoxide ions, the byproducts of oxygen metabolism in aerobic cells, are considered the main radical involved in oxidative damage^{21–23}. SOD can effectively dismutate the superoxide anions and has a key role in detoxifying free radicals, protecting cells from oxidative damage²⁴. Figure 3f shows the relative cell viability after incubation with nSOD and exposure to paraquat (an intracellular superoxide generating compound) for 12 h. The nanocapsules effectively protect the cells from oxidative injury at low concentrations. Increasing nanocapsule concentration, however, lowers the cell viability, which may be due to the increasing levels of hydroxyl radicals produced at high concentrations of SOD²¹. Nonetheless, this work further proves the potential use of nanocapsules for therapies and anti-aging applications.

Using the non-degradable nanocapsule platform, we have demonstrated that proteins for small molecular substrates can be effectively delivered with long-term stability and high activity. For macromolecular substrates, however, the polymer skin may prohibit their access to the core protein. It is well known that serum and late endosomes have pH values of ~ 7.4 and ~ 5.5 , respectively. Acid-degradable nanocapsules were therefore developed to overcome this obstacle. Using *de*-nCAS and nCAS as examples, we first studied their size evolution at pH 5.5 (Fig. 4a) and 7.4 (Fig. 4b). nCAS is stable at both values of pHs, but *de*-nCAS is only stable at pH 7.4. At pH 5.5, the average diameter of *de*-nCAS rapidly decreases within 3 h from 20 to 6 nm, a size similar to that of native CAS (~ 6 nm). Importantly, the degradable nanocapsules are stable against trypsin and α -chymotrypsin at pH 7.4 (Fig. 4c), which allows the degradable nanocapsules to remain stable in the circulation system, to be degraded when inside endosomes to release their protein cargoes intracellularly.

To further quantify the intracellular degradation, *de*-nEGFP and nEGFP were delivered to HeLa cells. The cellular fluorescence

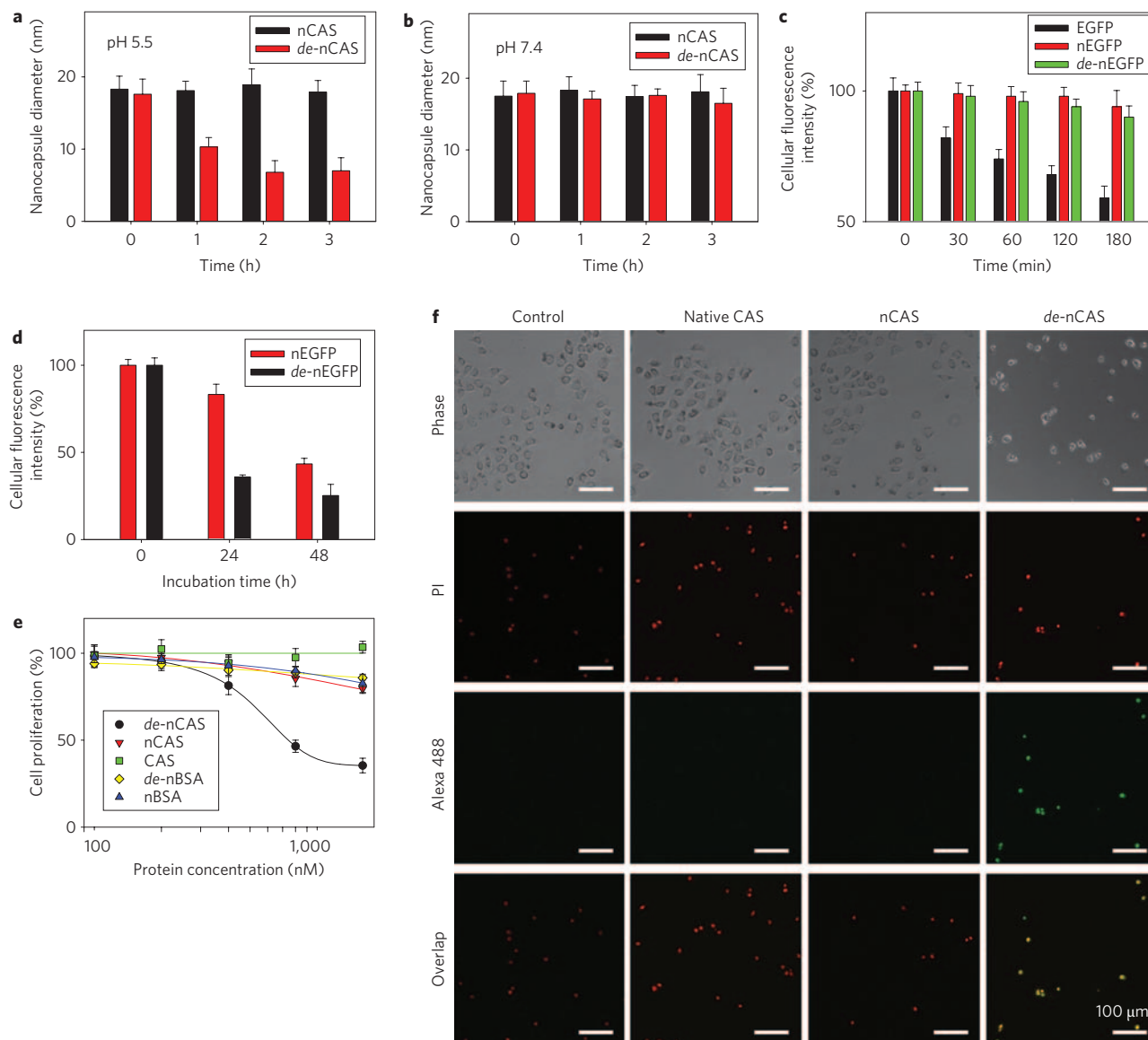


Figure 4 | Degradable nanocapsules. **a, b**, Sizes of degradable CAS nanocapsules (*de*-nCAS) and non-degradable CAS nanocapsule (nCAS) at pH 5.5 (**a**) and pH 7.4 (**b**). **c**, Fluorescence intensity of native EGFP, non-degradable EGFP nanocapsules (nEGFP) and degradable EGFP nanocapsules (*de*-nEGFP) after exposure to 1 mg ml⁻¹ trypsin and α -chymotrypsin in pH 7.4 buffer at 50 °C. Fluorescence intensities are normalized to native EGFP before addition of proteases. **d**, Fluorescence intensity of HeLa cells at different times after incubation with nEGFP or *de*-nEGFP for 3 h followed by incubation in fresh media. Fluorescence intensities are normalized to the respective cells that received no further incubation with fresh media. **e**, MTT assay showing the cell proliferation profile after incubation with various concentrations of *de*-nCAS, nCAS, CAS, *de*-nBSA or nBSA for 48 h. Data are normalized to untreated cells. **f**, APO-BrdUTM TUNEL assay showing HeLa cells transfected with native CAS, nCAS or *de*-nCAS. PI-stained nuclei (red) and Alexa Fluor 488-stained nick end label (green) in cells incubated with *de*-nCAS show apoptotic DNA fragmentation. Data represent averages, with error bars from three independent experiments performed in triplicate.

intensities of the cells with *de*-nEGFP are significantly lower than those with nEGFP after 24 h (Fig. 4d), confirming that degradable nanocapsules can be stripped of their shells in response to the acidic intercellular environment. Although a de-protection process inevitably exposes the cargo proteins to protease attack, it enables their interaction with large substrates. For example, CAS, a member of the cysteine protease family that plays an essential role in apoptosis, necrosis and inflammation, cleaves other protein substrates within the cells to trigger apoptosis^{25–27}. As shown in Fig. 4e, incubation of HeLa cells with native CAS, nCAS, *de*-nBSA or nBSA demonstrates similar viabilities that are significantly higher than those with *de*-nCAS. Terminal dUTP nick-end labelling (TUNEL) assay (Fig. 4f) confirms the apoptosis triggered by *de*-nCAS.

Unambiguously, this work demonstrates the effective delivery of proteins while maintaining their interaction with large substrates, bringing us a step closer to practical protein therapies.

To conclude, we have demonstrated a general, effective, low-toxicity intracellular protein delivery system based on single-protein nanocapsules. This work opens a new direction for cellular imaging, cancer therapies, anti-aging, cosmetics and many other applications. Further work on more robust, non-degradable nanocapsules for large molecular substrates is under way.

Methods

EGFP and TAT-EGFP fusion proteins were expressed according to previous reports²⁸. Fusion proteins were expressed in transformed *Escherichia coli* BL21 and

purified using a nickel-resin affinity column (Sigma Aldrich). The concentration of EGFP was determined by an extinction coefficient of $53,000 \text{ M}^{-1} \text{ cm}^{-1}$ at 489 nm. A volume of 10 mg EGFP in 3.8 ml of pH 8.5, 50 mM sodium carbonate buffer was reacted with 4 mg *N*-acryloxysuccinimide in 40 μl dimethyl sulphoxide (DMSO) for 2 h at room temperature. Finally, the reaction solution was thoroughly dialysed against pH 7.0, 20 mM phosphate buffer. The degrees of modification were measured using matrix-assisted laser desorption/ionization-time of flight (MALDI-TOF) mass spectra, which were varied from 5 to 20 vinyl groups per protein (Supplementary Fig. S7, Table S2). Using 5 ml acryloylated EGFP solution at 1 mg ml^{-1} , radical polymerization from the surface of the acryloylated protein was initiated by adding 2 mg ammonium persulphate dissolved in 30 μl deoxygenated and deionized water and 4 μl *N,N,N',N'*-tetramethylethylenediamine into the test tube. A specific amount of 2-dimethylaminoethyl methacrylate, acrylamide and *N,N'*-methylene bisacrylamide or glycerol dimethacrylate (molar ratio = 5:5:1) dissolved in 0.5 ml deoxygenated and deionized water was added to the test tube over 60 min. The reaction was allowed to proceed for another 60 min in a nitrogen atmosphere. Finally, dialysis was used to remove monomers and initiators. As-synthesized EGFP nanocapsules show similar fluorescent spectra to those of native EGFP (Supplementary Fig. S8). The yield of the protein nanocapsules was higher than 95%. The unmodified EGFP was removed using size-exclusion chromatography.

Syntheses of SOD, CAS, HRP, NIR-667-labelled-BSA and rhodamine-B-labelled-HRP nanocapsules were similar to that of EGFP nanocapsules. NIR-667-labelled BSA and rhodamine-B-labelled HRP were synthesized by modifying the proteins using a conjugating technique. CAS was expressed and purified using a method similar to that of EGFP; the plasmid used, pHC332, was a generous gift from Dr A. Clay Clark (North Carolina State University). Cu, Zn-SOD from bovine erythrocytes and horseradish peroxidase (Sigma-Aldrich) were used after dialysis against 20 mM pH 7.0 phosphate buffer. For the synthesis of HRP nanocapsules, 4-dimethylaminoantipyrine (1:10 weight ratio to HRP) was added into the reaction mixture as a stabilizer during acryloylation and polymerization steps. The synthesis and characterization of gold nanoparticle-labelled nanocapsules is provided in the Supplementary Information. Detailed information regarding nanocapsule synthesis, activity, stability, *in vitro* and *in vivo* studies are provided as Supplementary Information.

The characterization and *in vitro* and *in vivo* studies of the nanocapsules are described in detail in the Supplementary Information.

Received 10 August 2009; accepted 12 October 2009;
published online 22 November 2009

References

- Birch, J. R. & Onakunle, Y. in *Therapeutic Proteins, Methods and Protocols* 1–16 (Humana Press, 2005).
- Wadia, J. S., Becker-Hapak, M. & Dowdy, S. F. *Cell-Penetrating Peptides: Processes and Applications* 365 (CRC Press, 2002).
- Vyas, S. P., Singh, A. & Sihorkar, V. Ligand-receptor-mediated drug delivery: an emerging paradigm in cellular drug targeting. *Crit. Rev. Ther. Drug Carrier Syst.* **18**, 1–76 (2001).
- Sato, H., Sugiyama, Y., Tsuji, A. & Horikoshi, I. Importance of receptor-mediated endocytosis in peptide delivery and targeting: kinetic aspects. *Adv. Drug Deliv. Rev.* **19**, 445–467 (1996).
- Torchilin, V. P. Recent advances with liposomes as pharmaceutical carriers. *Nature Rev. Drug Discov.* **4**, 145–160 (2005).
- Bulmus, V. *et al.* A new pH-responsive and glutathione-reactive, endosomal membrane-disruptive polymeric carrier for intracellular delivery of biomolecular drugs. *J. Control Release* **93**, 105–120 (2003).
- Schwarze, S. R., Ho, A., Vocero-Akbani, A. & Dowdy, S. F. *In vivo* protein transduction: delivery of a biologically active protein into the mouse. *Science* **285**, 1569–1572 (1999).
- Heitz, F., Morris, M. C. & Divita, G. Twenty years of cell-penetrating peptides: from molecular mechanism to therapeutics. *Br. J. Pharmacol.* **157**, 195–206 (2009).
- Gros, E. *et al.* A non-covalent peptide-based strategy for protein and peptide nucleic acid delivery. *Biochim. Biophys. Acta* **1758**, 384–393 (2006).
- Fagain, C. O. Understanding and increasing protein stability. *Biochim. Biophys. Acta* **1252**, 1–14 (1995).
- Hooper, N. M. *Proteases in Biology and Medicine* (Portland Press, 2002).
- Brooks, H., Lebleu, B. & Vives, E. TAT peptide-mediated cellular delivery: back to basics. *Adv. Drug Deliv. Rev.* **57**, 559–577 (2005).
- Poon, G. M. K. & Garipey, J. Cell-surface proteoglycans as molecular portals for cationic peptide and polymer entry into cells. *Biochem. Soc. Trans.* **35**, 778–793 (2007).
- Futami, J. *et al.* Intracellular delivery of proteins into mammalian living cells by polyethylenimine-cationization. *J. Biosci. Bioeng.* **99**, 95–103 (2005).
- Fischer, R., Kohler, K., Fotin-Mlecsek, M. & Brock, R. A stepwise dissection of the intracellular fate of cationic cell-penetrating peptides. *J. Biol. Chem.* **279**, 12625–12635 (2004).
- Akinc, A., Thomas, M., Klivanov, A. M. & Langer, R. Exploring polymethylenimine-mediated DNA transfection and the proton sponge hypothesis. *J. Gene Med.* **7**, 657–663 (2004).
- Yamauchi, N. *et al.* Mechanism of synergistic cytotoxic effect between tumor-necrosis-factor and hyperthermia. *Jpn J. Canc. Res.* **83**, 540–545 (1992).
- Kaliberov, S. A. *et al.* Combination of cytosine deaminase suicide gene expression with DR5 antibody treatment increases cancer cell cytotoxicity. *Cancer Gene Ther.* **13**, 203–214 (2006).
- Folkes, L. K. & Wardman, P. Oxidative activation of indole-3-acetic acids to cytotoxic species — a potential new role for plant auxins in cancer therapy. *Biochem. Pharmacol.* **61**, 129–136 (2001).
- de Melo, M. P., de Lima, T. M., Pithon-Curi, T. C. & Curi, R. The mechanism of indole acetic acid cytotoxicity. *Toxicol. Lett.* **148**, 103–111 (2004).
- Fridovich, I. Superoxide radical: an endogenous toxicant. *Ann. Rev. Pharmacol. Toxicol.* **23**, 239–257 (1983).
- Finkel, T. & Holbrook, N. J. Oxidants, oxidative stress and the biology of aging. *Nature* **408**, 239–244 (2000).
- Ames, B. N., Shigenaga, M. K. & Hagen, T. M. Oxidants, antioxidants and the degenerative diseases of aging. *Proc. Natl Acad. Sci. USA* **90**, 7915–7922 (1993).
- McCord, J. M. Superoxide dismutase in aging and disease: an overview. *Methods Enzymol.* **349**, 331–341 (2002).
- Nicholson, D. W. *et al.* Identification and inhibition of the ICE/CED-3 protease necessary for mammalian apoptosis. *Nature* **376**, 37–43 (1995).
- Porter, A. G. & Janicke, R. U. Emerging roles of caspase-3 in apoptosis. *Cell Death Differ.* **6**, 99–104 (1999).
- Oliver, L. & Vallette, F. M. The role of caspases in cell death and differentiation. *Drug Resist. Updates* **8**, 163–170 (2005).
- Caron, N. J. *et al.* Intracellular delivery of a Tat-eGFP fusion protein into muscle cells. *Mol. Ther.* **3**, 310–318 (2001).

Acknowledgements

This work was partially supported by the Defense Threat Reducing Agency (DTRA), NSF-CAREER, Sandia National Laboratories and CheungKong Scholar Program through Tsinghua University, China.

Author contributions

M.Y., Z.L., T.S., Y.T. and Y.L. conceived and designed the experiments. M.Y., J.D. and Z.G. performed the experiments. Y.H., W.Z., L.W. and Z.H.Z. helped to analyse the data. Z.L., T.S., Y.T. and Y.L. co-wrote the paper. All authors discussed the results and commented on the manuscript.

Additional information

The authors declare no competing financial interests. Supplementary information accompanies this paper at www.nature.com/naturenanotechnology. Reprints and permission information is available online at <http://npg.nature.com/reprintsandpermissions/>. Correspondence and requests for materials should be addressed to Z.L., T.S., Y.T. and Y.L.